Microporous and Mesoporous Materials 288 (2019) 109580

Contents lists available at ScienceDirect

Microporous and Mesoporous Materials

journal homepage: www.elsevier.com/locate/micromeso

Real-time inline monitoring of zeolite synthesis by Photon Density Wave spectroscopy

Janick Häne[a], Dominik Brühwiler[b], Achim Ecker[a], Roland Hass[c,*]

[a] Centre of Industrial Chemistry and Processes, Institute of Chemistry and Biotechnology, Zürich University of Applied Sciences (ZHAW), CH-8820, Wädenswil, Switzerland
[b] Section of Polymer Chemistry, Institute of Chemistry and Biotechnology, Zürich University of Applied Sciences (ZHAW), CH-8820, Wädenswil, Switzerland
[c] Physical Chemistry – innoFSPEC Potsdam, University of Potsdam, D-14476, Potsdam-Golm, Germany

ARTICLE INFO

Keywords:
Photon density wave spectroscopy
Process analytical technology
Zeolite synthesis
Molar water content
Silica source

ABSTRACT

The formation process of zeolite A (Linde Type A) was monitored inline at 1.5 L scale by Photon Density Wave (PDW) spectroscopy as novel process analytical technology for highly turbid liquid suspensions. As a result, the reduced scattering coefficient, being a measure for particle number, size, and morphology, provides distinct process information, including the formation of amorphous particles and their transfer into crystalline zeolite structures. The onset and end of the crystallization process can be detected inline and in real-time. Analyses by powder X-ray diffraction and electron microscopy, based on a sampling approach, support the interpretation of the results obtained by PDW spectroscopy. In addition, the influence of the molar water content was investigated, indicating a linear increase of the time needed to reach the end of the zeolite A crystallization with increasing molar water content. Further experiments indicate a strong influence of the silica source on the course of the crystallization. The applicability of PDW spectroscopy under even more demanding chemical and physical conditions was investigated by monitoring the synthesis of zeolite L (Linde Type L).

1. Introduction

The first synthesis of a zeolite was reported by St. Claire Deville in 1862 for levynite [1]. Almost a century later, first industrial amounts of zeolites were made available by Union Carbide in 1954, providing a few hundred tons per year in the late 1950s [2]. Other companies such as Mobil Oil, Grace, and Henkel followed in the 1960s and 1970s [3]. Zeolite A, X, Y, and ZSM-5 are currently the commercially most important zeolites. The annual production of synthetic zeolites was estimated to $2{\cdot}10^6$ tons per year for 2009 [4].

In spite of the mega ton scale, the global multi-billion dollar market [4], and their diverse applications, synthetic zeolites are still produced or crystallized batch-wise without using inline process analytical technologies (PAT), apart from measuring temperature, pressure, or conductivity. The current analytical approaches for zeolites are based on offline, cost-intensive, and time-consuming techniques, such as element analysis, powder X-ray diffraction (XRD), scanning electron microscopy (SEM), physisorption characterization, and light scattering [5]. In many other sectors of the chemical industry, PAT are frequently applied [6–8] including crystallization process monitoring [9]. However, options for inline sub-micrometer particle or droplet sizing in concentrated systems are limited. In general, inline PAT has the potential to gain additional or faster process insight, to improve product quality (e.g., by quickly detecting process deviations), and to speed up production (e.g., by reducing cycle time and increasing space-time-yields) [6].

In the past, efforts to analyze the crystallization of zeolites in real-time have been undertaken on the lab scale with focus on mechanisms rather than particle size. Different analytical methods, such as electrochemical methods/conductivity [10,11], viscosity measurements [12], calorimetry [13], spectroscopic methods [14] (IR [15,16], Raman [17–19], NMR [20,21], X-Ray absorption (XANES, EXAFS) [22]), mass spectrometry [23], and X-ray powder diffraction (XRD) [24–26] as well as X-ray scattering (SAXS, WAXS) [22,27–29], have been employed. To the best of our knowledge, only two publications report on inline spectroscopic methods applicable in pilot or production scale (IR spectroscopy [30], Raman spectroscopy [31]), whereas all others are based on specially designed at-/off-line measurement cells or sampling approaches for zeolite characterization.

The real-time, inline or online characterization of zeolite syntheses is intrinsically challenging due to the typical processing conditions, i.e., high temperatures (often above 150 °C), high alkalinity (often pH ≈ 14), high turbidity (intrinsic to crystallizations), strong stirring, and a potentially high degree of inhomogeneity, as well as concerns of material deposition on process probes (so-called probe fouling).

* Corresponding author.
E-mail address: rhass@uni-potsdam.de (R. Hass).

https://doi.org/10.1016/j.micromeso.2019.109580
Received 1 March 2019; Received in revised form 26 June 2019; Accepted 27 June 2019
Available online 28 June 2019

In this work, a novel approach to monitor zeolite synthesis inline and in real-time by means of Photon Density Wave (PDW) spectroscopy [32–35] is reported. PDW spectroscopy is an inline PAT capable of calibration-free quantification of light absorption and light scattering in highly turbid, highly concentrated liquid suspensions, even under strong stirring conditions. The experimental results are expressed as absorption coefficient (μ_a) and reduced scattering coefficient (μ_s'), being the absolute optical properties of the turbid material. While μ_a is linked to the chemical composition (Lambert-Beer law) of the suspension, μ_s' is linked to the size, concentration, and morphology of the suspended particles. Recently, PDW spectroscopy has been applied successfully to cooling crystallization processes prone to process probe fouling with mass fractions of 60% [36].

Based on Mie theory [37] and theories for so-called dependent light scattering [32], particle sizes can be obtained from the reduced scattering coefficient. However, here the focus is put on the systematic evaluation of the fundamental applicability of PDW spectroscopy with respect to the monitoring of the optical properties during the synthesis of zeolite A (Linde Type A, LTA). In addition, first experiments using PDW spectroscopy during zeolite L (Linde Type L, LTL) synthesis were performed, representing even more challenging process conditions.

2. Experimental

2.1. Materials

Sodium aluminate anhydrous (technical), sodium hydroxide (≥98%), LUDOX® HS-40 colloidal silica (40 wt%), and tetraethyl orthosilicate (TEOS, ≥ 99.0%, GC) were purchased from Sigma-Aldrich. Aerosil® OX-50 (100%) was purchased from Evonik Industries. Sodium metasilicate pentahydrate (pure) and nitric acid (65%) were obtained from Carl Roth. The purity of sodium metasilicate pentahydrate was assumed to be 100%. For further calculations, the composition of the sodium aluminate was taken from the certificate of analysis (57% Al_2O_3, 38% Na_2O). All chemicals were used as received.

2.2. Zeolite synthesis

For the synthesis of **zeolite A** a verified procedure was followed [38]. Sodium hydroxide was dissolved in 850 mL of ultrapure water (conductivity 0.055 µS/cm). Half of the sodium hydroxide solution was used to dissolve the sodium metasilicate pentahydrate (silica solution). Sodium aluminate was dissolved in the other half of the sodium hydroxide solution (aluminate solution). The aluminate solution was then filtered by means of a cellulose filter (Whatman Grade 2) and vacuum to obtain a visually clear solution. The loss of water was compensated accordingly. The aluminate solution was transferred into a 1.5 L stainless steel autoclave with PTFE inliner (ecoclave Type 3, 1.5 L, Büchi AG, Uster, Switzerland) and stirred with 500 rpm at 25 °C using a PTFE propeller with three 45° angular blades (BOLA Propeller Stirrer Shaft C 378, Bohlender GmbH, Grünsfeld, Germany). After reaching 25 °C, inline monitoring with PDW spectroscopy and recording of the relative torque of the stirrer was initiated. After another 5 min, the silica solution was added within 1 min. The molar composition of the resultant reaction mass was 3.165 Na_2O: 1.00 Al_2O_3: 1.926 SiO_2: x H_2O with varying molar water content (x = 128, 200, 250, and 300 mol H_2O per mole of Al_2O_3). The reaction mass was stirred for 5 min at 25 °C, then the jacket temperature of the autoclave was set to 100 °C. The reaction time was varied between 3 and 20 h. The reaction mass was subsequently allowed to cool to 30 °C before filtration. After filtration, the zeolite was washed with boiling ultrapure water until the filtrate reached a pH < 9. The material was dried overnight under vacuum (100 mbar) at 80 °C. The procedure for the synthesis of **zeolite L** is described in the Supplementary Information.

For offline analysis, 10 mL samples were directly taken out of the reactor by means of a plastic pipette and were added to 40 mL of cold ultrapure water. The suspension was immediately filtered and the solid was washed with ultrapure water until the washing solution reached pH ≈ 8. After each synthesis, the PDW spectroscopy process probe as well as the reactor were cleaned overnight with 1 mol/L of nitric acid at 25 °C. The entire system was then rinsed with ultrapure water until the washing solution reached pH 7.

2.3. Photon Density Wave (PDW) spectroscopy

PDW spectroscopy is a light scattering technique based on photon transport theory in multiple light scattering environments and is therefore especially suitable for highly turbid systems. Experimentally, intensity-modulated light is inserted with an optical fiber acting as a point-like light source in a strongly light scattering and weakly absorbing material, such as a zeolite suspension. Due to absorption and multiple scattering of the intensity modulated light, a PDW is created inside this suspension. As function of emitter/detector-fiber distance and modulation frequency, shifts of the amplitude and the phase of the PDW are characterized experimentally. More details on the theoretical background are found elsewhere [32].

The PDW spectrometer is self-built. The most relevant parts consist of a vector network analyzer (VNA) (ZNB4, Rohde & Schwarz GmbH & Co. KG, Munich, Germany) as main analytic tool. The VNA generates a sinusoidal electrical high-frequency signal, which is combined with the laser current via a BIAS-T (ZFBGT4R2GW, Minicircuits, Brooklyn, NY, USA) to generate a high frequency modulated laser current. Thus, the laser diodes (e.g., from Thorlabs GmbH, Dachau/Munich, Germany) emit intensity-modulated light, which is coupled into an optical fiber (HCPM0600T, Laser Components GmbH, Olching, Germany) and guided into the suspension (emission fiber). Seven detection fibers, each positioned in different distance to the emission fiber, are integrated in a custom-made stainless steel process probe of 25 mm diameter. A photograph of such a process probe is shown elsewhere [36]. The detection fibers guide light out of the suspension and onto an avalanche photo diode (APM-400P, Becker & Hickl GmbH, Berlin, Germany) as detector. The resulting signal is then analyzed by the VNA with respect to changes in phase and amplitude. The general setup concept of a PDW spectrometer is depicted elsewhere [32]. The spectrometers currently are of a similar dimension as a "mobile file cabinet" and the process probe is equipped with an approx. 10 m fiber optical conduit to spatially decouple the spectrometer and the process probe.

As experimental parameters, two different wavelengths of λ = 636 and 914 nm were used in consecutive measurements. 41 modulation frequencies within the typical range of 10–310 MHz and 7 fiber distances within the typical range of 5–13 mm were characterized.

Functionality and performance of the PDW spectroscopy process probe were tested after each synthesis. For this purpose, the optical fibers were visually inspected for damage and a photographic image of the process probe was taken for comparison. The performance of the process probe was checked by measuring commercially available milk with 3.5% fat [39]. Significant damages typically cause off-target optical coefficients for the milk sample. No such damages were observed after the zeolite A syntheses.

For the determination of the optical coefficients during zeolite synthesis, an estimation of the refractive index and the density is sufficient for PDW spectroscopy raw data analysis. A refractive index n = 1.45 and density $\rho = 1.99\ g\ cm^{-3}$ [40] was used for zeolite. Once particle size analysis will be developed for zeolite synthesis, these parameters need to be characterized in more detail.

2.4. Characterization of zeolite samples

Powder X-ray diffraction (XRD) data was collected on a diffractometer (STOE STADI P, STOE & Cie GmbH, Darmstadt, Germany) in transmission mode with a Ge monochromator and MoKα radiation. The resulting diffractograms of the zeolite A samples were compared

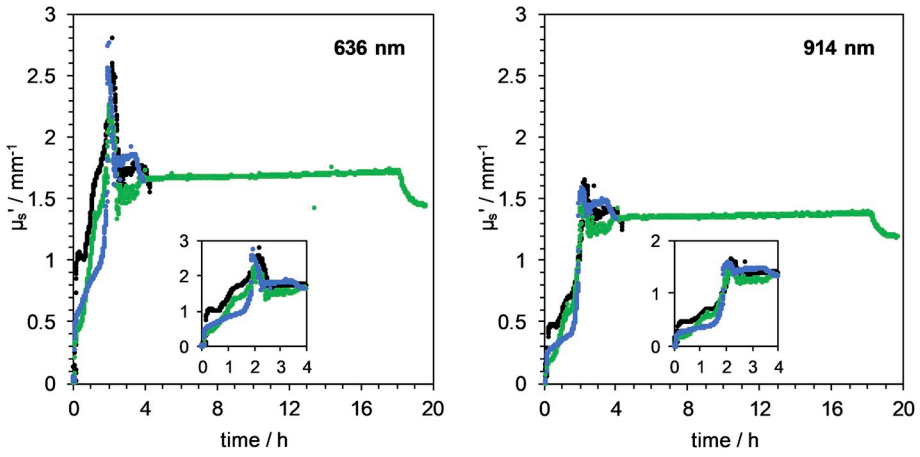

Fig. 1. Inline monitoring of three equivalent zeolite A syntheses with PDW spectroscopy. The diagrams show the reduced scattering coefficients μ_s' at laser wavelengths of 636 nm (left) and 914 nm (right). The first 4 h of the syntheses are displayed in the respective insets. The molar composition was 3.165 Na_2O: 1.00 Al_2O_3: 1.926 SiO_2: 128 H_2O. Identical control parameters were used for the three syntheses. The respective process data is given in Fig. S1.

with the IZA database [41]. Scanning electron microscopy (SEM) images (FEI Quanta FEG 250, FEI Company, Hillsboro, USA) were collected after sputtering the samples with gold.

3. Results and discussion

3.1. Zeolite A syntheses monitored by inline PDW spectroscopy

Fig. 1 displays the reduced scattering coefficient μ_s' observed during the course of three equivalent zeolite A syntheses. All three syntheses show a similar temporal development of μ_s' at both laser wavelengths, with the μ_s' value being higher at 636 nm. This is in agreement with the typical light scattering properties of particles [33]. These results indicate that zeolite A syntheses can be monitored with PDW spectroscopy inline and in real-time. It is essential to accompany inline data with process data (see Supplementary Information). Examination of the process data reveals differences between the three syntheses, which might explain the slightly different development of μ_s' during the first hours. PDW spectroscopy is in general a method of high precision, based on referencing against light scattering theory and other particle sizing methods [32,33]. For the processes investigated here, also the absorption coefficients μ_a display changes and variations at both wavelengths within these first hours of synthesis (Fig. S2). It needs to be evaluated in more detail to what extent process variations can be limited by improved process development and if such improvements would be reflected also by the optical coefficients. In the following however, only the results for the reduced scattering coefficient obtained at 636 nm are discussed, because the light scattering effects are more pronounced at shorter wavelength and a relation to offline reference analysis is intended. The following interpretation of the development of the reduced scattering coefficient during zeolite A formation is based on common behaviour of light scattering in concentrated suspensions and supported by offline reference data from SEM and XRD. A complete interpretation of μ_s' would require model development which is not within the scope of the present work.

The reduced scattering coefficient μ_s' increases rapidly at the start of the synthesis. This is due to the particle formation and the concomitant increase of turbidity in the reaction mass when adding the silica solution to the aluminate solution. Initially, μ_s' increases constantly for about 1.2 h, followed by an even faster increase until reaching a maximum after approximately 2 h. This increase is connected to the particle formation and growth, until a critical point in time at which light scattering starts to decrease rapidly. This critical time is interpreted as the start of crystallization and is therefore referred to as **crystallization onset** (CO). The CO is followed by a rapid decrease of μ_s' to a constant level, which does not change until the reaction mass is cooled. A constant value of μ_s' implies that no change in particle size, number, and shape occurs, thus indicating the end of the zeolite formation. The point in time at which μ_s' starts to remain constant can be referred to as the **crystallization end** (CE). For the investigated experimental conditions, the CO occurred after about 2 h and the CE after about 3.5 h (Fig. 1). To provide evidence that the formation of zeolite A crystals begins with the CO, six samples (S1 to S6) were collected for analysis by SEM and XRD. The reduced scattering coefficient as a function of time and the sampling points are shown in Fig. 2 with a SEM image of the final product after a synthesis time of 20 h. SEM images of the in-process samples S1 to S6 are displayed in Fig. 3.

The SEM images of the samples S1 to S3 only show small agglomerated alumosilicate particles. The first larger particles with the typical cubic shape of zeolite A crystals can be seen on the SEM image of

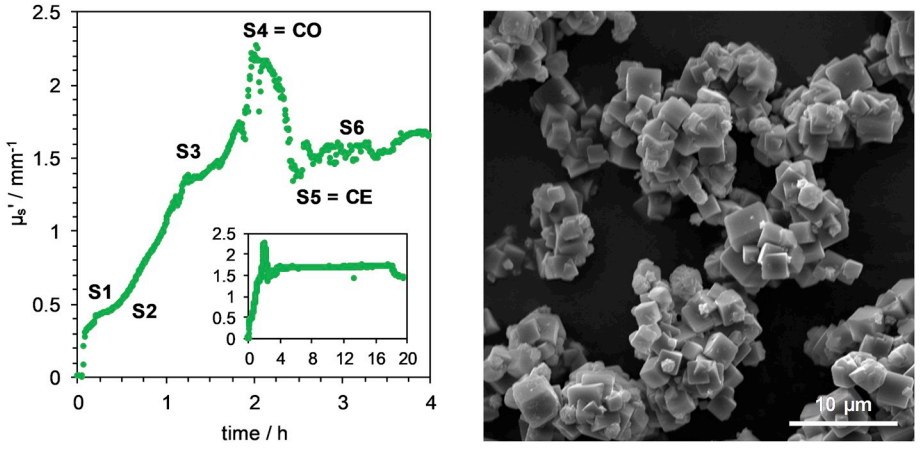

Fig. 2. Left: Reduced scattering coefficient μ_s' at 636 nm during the first 4 h of the zeolite A synthesis (inset: entire duration). Samples were taken after 0.25 h (S1), 0.75 h (S2), 1.25 h (S3), 2 h (S4), 2.67 h (S5), and 3.08 h (S6), with S4 approximatively representing the crystallization onset (CO) and S5 the crystallization end (CE). Right: SEM image of the final product obtained after 20 h of synthesis time.

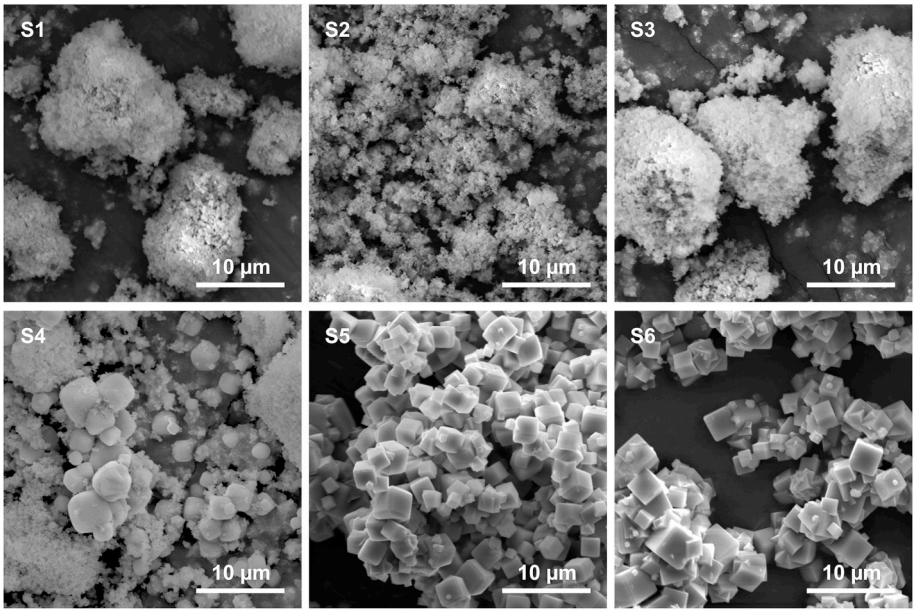

Fig. 3. SEM images of the six collected in-process samples according to Fig. 2 after 0.25 h (S1), 0.75 h (S2), 1.25 h (S3), 2 h (S4), 2.67 h (S5), and 3.08 h (S6).

sample S4. The in-process sample S4 was taken at the point associated with the CO when μ_s' reached its maximum value. These observations support the hypothesis that the zeolite A formation features a specific delayed onset and is not directly initiated when mixing the silica and aluminate solutions [42,43]. Sample S5 was taken after μ_s' remained constant and may be attributed to the CE. Only cubic zeolite A crystals can be identified in the SEM image of sample S5, indicating that the crystal formation is indeed completed when μ_s' reaches a constant value. This is further supported by the SEM image of sample S6, which exclusively shows cubic zeolite A crystals. The initial formation of spherical amorphous alumosilicate particles from which the zeolite A crystals are formed after a certain period of time has been described previously [42,43].

An explanation for the decrease of μ_s' after the peak at the CO might be the reduced number and larger size of the particles due to the zeolite formation in comparison to the small-scale alumosilicate particles. With respect to μ_s' of a suspension having a given mass fraction, such larger particles scatter light less than the smaller particles. Depending amongst other factors on refractive indices, mass fractions, and wavelength, this effect starts to occur for particle diameters larger than half of the experimental wavelength [33]. The drop in light scattering observed here may represent the transformation of amorphous particles to zeolite A crystals.

Further evidence for the transformation from amorphous to crystalline structure for these particular samples S1 to S6 is provided by powder XRD data (Fig. 4). For the samples S1 to S3, the diffractograms do not contain any specific reflections. For sample S4 the distinctive reflections of zeolite A are already visible and thus can be attributed to the CO.

Inline monitoring of zeolite synthesis is generally difficult due to high turbidity and high alkalinity in combination with high temperature. To evaluate the stability of the PDW spectroscopy process probe, tests were run after each synthesis. Even after more than 20 zeolite A syntheses lasting about 200 h overall, no damages to the probe were found, both visually and in terms of performance during the tests with milk samples.

3.2. Effect of water content and silica source on zeolite A crystallization

In another set of experiments the effect of the molar water content was evaluated while keeping the volume of the reaction mass constant.

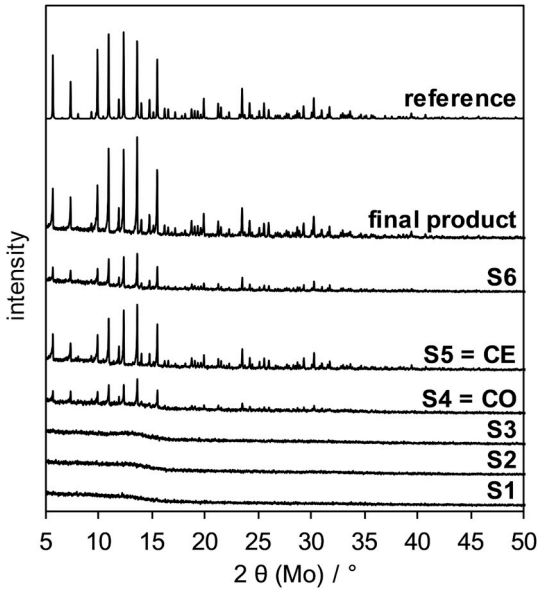

Fig. 4. Powder XRD patterns of in-process samples S1 to S6 and of the final product. The patterns are offset for clarity. A reference pattern for hydrated zeolite A [48] is shown for comparison.

The experiments summarized in Fig. 5 show the progression of μ_s' for different water contents. It can be observed that the temporal development with respect to the sharp peak as seen in Fig. 1 changes. Instead of this peak, rather longer lasting plateaus at maximal light scattering are observed per level of molar water content. For the molar water content of x = 128, 200, and 250 mol of H_2O per mole of Al_2O_3, the maximal reduced scattering coefficient decreases in this order. A tentative interpretation could be a longer existence of amorphous precursor particles, causing an increased delay of the transformation into crystalline zeolite structures. Here, with increasing molar water content, the CE is delayed. If the time to reach the CE is plotted as a function of the molar water content (Fig. 5, right), a linear trend is observed. According to XRD data, zeolite A was obtained in all six syntheses. For a molar water content of x = 300 mol of H_2O per mole of Al_2O_3 a secondary crystalline phase was detected. The decrease of the

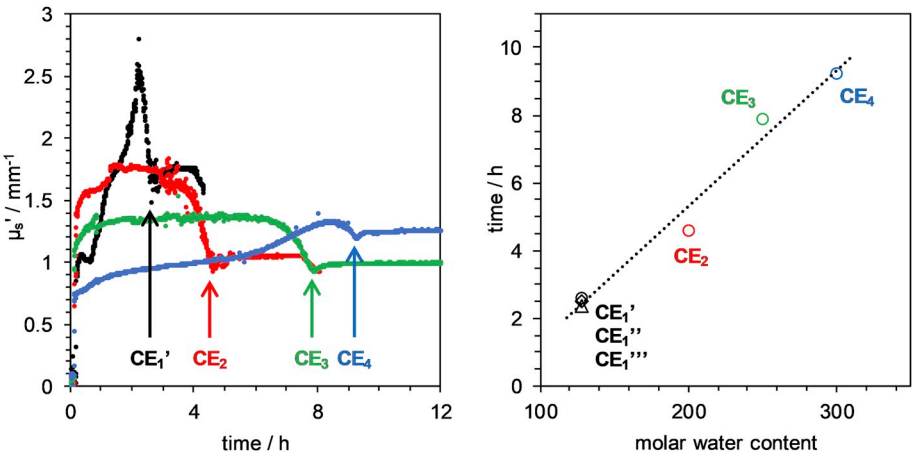

Fig. 5. Left: Reduced scattering coefficient μ_s' at 636 nm during zeolite A synthesis as a function of time for different molar water contents: 3.165 Na_2O: 1.00 Al_2O_3: 1.926 SiO_2: x H_2O, where x = 128 (black), 200 (red), 250 (green), and 300 (blue). Right: Time to reach CE as a function of molar water content. The values of CE_1', CE_1'', and CE_1''', corresponding to three equivalent syntheses, indicate good reproducibility of CE determination. (For interpretation of the references to colour in this figure legend, the reader is referred to the Web version of this article.)

signal intensity of μ_s' with increasing molar water content is based on the reduced amount of solid content, since the volume of the reaction mass was kept constant throughout all syntheses. It is known from previous studies that the crystallinity is influenced by the amount of water [44,45]. However, to our knowledge, a linear trend of CE with respect to the molar water content has not yet been observed.

Another well-known factor determining the outcome of a zeolite synthesis is the type of silica source [46]. To evaluate if real-time inline PDW spectroscopy observes such effects during synthesis, different silica sources (Aerosil® OX-50, TEOS, Ludox HS 40, and sodium metasilicate pentahydrate) were employed. The composition of the reaction mass was set to 3.165 Na_2O: 1.00 Al_2O_3: 1.926 SiO_2: 128 H_2O as described in the experimental section. The different silica sources led to pronounced differences regarding the course of μ_s' during the synthesis. The results are displayed in Fig. S3.

3.3. Zeolite L synthesis monitored by inline PDW spectroscopy

The synthesis of zeolite L (Linde Type L, LTL) represents even more chemically and physically challenging conditions for inline PAT [47]. Pressure (6 bar), temperature (160 °C), alkalinity (pH 14), and duration (42 h) pose significant challenges for the optical components of process probes for inline spectroscopy. First results indicate that zeolite L syntheses can be monitored by inline PDW spectroscopy in real-time (see Supplementary Information). However, after a few syntheses, the optical fibers of the process probe started to deteriorate (glass dissolution due to high pH, temperature, and pressure) so that data of decreasing quality were obtained. Either a process probe suitable for the demands of PDW spectroscopy and suitable for the conditions of zeolite L synthesis have to be developed or a "single use" approach for the process probe needs to be adopted.

4. Conclusions

Photon Density Wave (PDW) spectroscopy is suitable for real-time inline monitoring of zeolite synthesis, showing characteristic trends of the reduced scattering coefficient for different systems. The data obtained for the synthesis of zeolite A suggests that small spherical amorphous alumosilicate particles form quickly after mixing of the silica and aluminate solutions. These particles are transformed to zeolite A crystals after a certain amount of time. The onset of the zeolite A crystallization is, according to first indications, the moment at which the system exhibits maximum light scattering. Due to the formation of zeolite A crystals, the reduced scattering coefficient subsequently decreases rapidly and reaches a constant value. It is assumed that the crystallization is complete after reaching a constant reduced scattering coefficient.

A linear trend of the time to reach the end of zeolite A crystallization (CE) in dependence of the molar water content was observed. The results obtained so far provide a promising basis for further experiments regarding inline monitoring of zeolite syntheses. In particular, future work will need to focus on the model development for inline particle size analysis based on the reduced scattering coefficient from PDW spectroscopy.

The ability of PDW spectroscopy to determine the endpoint of zeolite synthesis in real-time has the potential to reduce cycle time, increase space-time-yield, and avoid time-consuming in-process sampling. In an industrial context, reduction of cycle time means reduction of operational cost (increasing margin) or additional capacity (avoiding investment). Considering the mega ton scale of annual zeolite production, inline PDW spectroscopy thus can influence the efficiency of industrial zeolite production.

Acknowledgements

This work was supported by the German Federal Ministry of Education and Research (grant 03Z22AN12). The authors thank the group of Prof. Dr. Greta Patzke (University of Zurich) for powder XRD measurements.

Appendix A. Supplementary data

Supplementary data to this article can be found online at https://doi.org/10.1016/j.micromeso.2019.109580.

Declaration of interest

None.

References

[1] R.W. Broach, D.-Y. Jan, D.A. Lesch, S. Kulprathipanja, E. Roland, P. Kleinschmit, Zeolites, Ullmann's Encycl. Ind. Chem. (2012) 1–35, https://doi.org/10.1002/14356007.a28_475.pub2.
[2] E. Roland, Industrial production of zeolites, Stud. Surf. Sci. Catal. 46 (1989) 645–659 https://doi.org/10.1016/S0167-2991(08)61019-8.
[3] E.M. Flanigen, R.W. Broach, S.T. Wilson, Introduction, in: S. Kulprathipanja (Ed.), Zeolites in Industrial Separation and Catalysis, Wiley-VCH Verlag GmbH & Co. KGaA, Weinheim, Germany, 2010, pp. 1–26, , https://doi.org/10.1002/9783527629565.ch1.
[4] Stratistics MRC, Zeolite - Global Market Outlook (2017-2026), (2018) https://www.strategymrc.com/report/zeolite-market , Accessed date: 23 January 2019.
[5] Zeochem AG/Uetikon Switzerland, Grace GmbH/Worms Germany (2018), Arkema SA/Colombes France (2018), Personal Communication Concerning PAT for Zeolite Production, (2015).
[6] R.W. Kessler (Ed.), Prozessanalytik: Strategien und Fallbeispiele aus der industriellen Praxis, Wiley-VCH Verlag GmbH & Co. KGaA, Weinheim, FRG, 2006.
[7] K.A. Bakeev (Ed.), Process Analytical Technology: Spectroscopic Tools and Implementation Strategies for the Chemical and Pharmaceutical Industries, Second ed., John Wiley & Sons, Ltd, 2010, http://doi.wiley.com/10.1002/9780470689592.

[8] L.L. Simon, H. Pataki, G. Marosi, F. Meemken, K. Hungerbühler, A. Baiker, S. Tummala, B. Glennon, M. Kuentz, G. Steele, H.J.M. Kramer, J.W. Rydzak, Z. Chen, J. Morris, F. Kjell, R. Singh, R. Gani, K.V. Gernaey, M. Louhi-Kultanen, J. O'Reilly, N. Sandler, O. Antikainen, J. Yliruusi, P. Frohberg, J. Ulrich, R.D. Braatz, T. Leyssens, M. von Stosch, R. Oliveira, R.B.H. Tan, H. Wu, M. Khan, D. O'Grady, A. Pandey, R. Westra, E. Delle-Case, D. Pape, D. Angelosante, Y. Maret, O. Steiger, M. Lenner, K. Abbou-Oucherif, Z.K. Nagy, J.D. Litster, V.K. Kamaraju, M.-S. Chiu, Assessment of recent process analytical technology (PAT) trends: a multiauthor review, Org. Process Res. Dev. 19 (2015) 3–62, https://doi.org/10.1021/op500261y.

[9] L.L. Simon, E. Simone, K. Abbou Oucherif, Crystallization process monitoring and control using process analytical technology, Computer Aided Chemical Engineering, Elsevier, 2018, pp. 215–242, , https://doi.org/10.1016/B978-0-444-63963-9.00009-9.

[10] M. Tatlıer, M. Elnekave, Electrochemical monitoring of zeolite synthesis, Mater. Chem. Phys. 91 (2005) 99–103, https://doi.org/10.1016/j.matchemphys.2004.10.055.

[11] G. Cao, M.J. Shah, In situ monitoring of zeolite crystallization by electrical conductivity measurement: New insight into zeolite crystallization mechanism, Microporous Mesoporous Mater. 101 (2007) 19–23, https://doi.org/10.1016/j.micromeso.2006.12.011.

[12] L.R.A. Follens, E.K. Reichel, C. Riesch, J. Vermant, J.A. Martens, C.E.A. Kirschhock, B. Jakoby, Viscosity sensing in heated alkaline zeolite synthesis media, Phys. Chem. Chem. Phys. 11 (2009) 2854–2857, https://doi.org/10.1039/B816040F.

[13] S. Yang, A. Navrotsky, B.L. Phillips, In situ calorimetric, structural, and compositional study of zeolite synthesis in the system $5.15Na_2O-1.00Al_2O_3-3.28SiO_2-165H_2O$, J. Phys. Chem. B 104 (2000) 6071–6080, https://doi.org/10.1021/jp9944278.

[14] A. Aerts, C.E.A. Kirschhock, J.A. Martens, Methods for in situ spectroscopic probing of the synthesis of a zeolite, Chem. Soc. Rev. 39 (2010) 4626–4642, https://doi.org/10.1039/B919704B.

[15] M.T. Sánchez, J. Pérez-Pariente, C. Márquez-Alvarez, In situ ATR-FTIR for monitoring the kinetics of mesoporous molecular sieves synthesis, Stud. Surf. Sci. Catal. 158 A (2005) 113–120, https://doi.org/10.1016/S0167-2991(05)80329-5.

[16] C.J. Van Oers, K. Góra-Marek, K. Sadowska, M. Mertens, V. Meynen, J. Datka, P. Cool, In situ IR spectroscopic study to reveal the impact of the synthesis conditions of zeolite β nanoparticles on the acidic properties of the resulting zeolite, Chem. Eng. J. 237 (2014) 372–379, https://doi.org/10.1016/j.cej.2013.10.041.

[17] G. Xiong, Y. Yu, Z. Feng, Q. Xin, F.-S. Xiao, C. Li, UV Raman spectroscopic study on the synthesis mechanism of zeolite X, Microporous Mesoporous Mater. 42 (2001) 317–323, https://doi.org/10.1016/S1387-1811(00)00340-1.

[18] F. Fan, Z. Feng, G. Li, K. Sun, P. Ying, C. Li, In situ UV Raman spectroscopic studies on the synthesis mechanism of zeolite X, Chem. Eur J. 14 (2008) 5125–5129, https://doi.org/10.1002/chem.200800560.

[19] T.F. Chaves, F.L.F. Soares, D. Cardoso, R.L. Carneiro, Monitoring of the crystallization of zeolite LTA using Raman and chemometric tools, Analyst 140 (2015) 854–859, https://doi.org/10.1039/C4AN00913D.

[20] J. Shi, M.W. Anderson, S.W. Carr, Direct observation of zeolite a synthesis by in situ solid-state NMR, Chem. Mater. 8 (1996) 369–375, https://doi.org/10.1021/cm950028n.

[21] M. Haouas, Nuclear magnetic resonance spectroscopy for in situ monitoring of porous materials formation under hydrothermal conditions, Materials 11 (2018) 1416–1434, https://doi.org/10.3390/ma11081416.

[22] M.G. O'Brien, A.M. Beale, B.M. Weckhuysen, The role of synchrotron radiation in examining the self-assembly of crystalline nanoporous framework materials: from zeolites and aluminophosphates to metal organic hybrids, Chem. Soc. Rev. 39 (2010) 4767–4782, https://doi.org/10.1039/C0CS00088D.

[23] S.A. Pelster, R. Kalamajka, W. Schrader, F. Schüth, Monitoring the nucleation of zeolites by mass spectrometry, Angew. Chem. Int. Ed. 46 (2007) 2299–2302, https://doi.org/10.1002/anie.200604513.

[24] P. Norby, Hydrothermal conversion of zeolites: an *in situ* synchrotron X-ray powder diffraction study, J. Am. Chem. Soc. 119 (1997) 5215–5221, https://doi.org/10.1021/ja964245g.

[25] R. Grizzetti, G. Artioli, Kinetics of nucleation and growth of zeolite LTA from clear solution by in situ and ex situ XRPD, Microporous Mesoporous Mater. 54 (2002) 105–112, https://doi.org/10.1016/S1387-1811(02)00357-8.

[26] P. Norby, In-situ XRD as a tool to understanding zeolite crystallization, Curr. Opin. Colloid Interface Sci. 11 (2006) 118–125, https://doi.org/10.1016/j.cocis.2005.11.003.

[27] R. Grizzetti, G. Artioli, M. Gemmi, F. Carsughi, P. Riello, In situ WAXS-SAXS synchrotron study of the kinetics of nucleation and growth in Linde type-A zeolite (LTA), Stud. Surf. Sci. Catal. 154 (Part A) (2004) 355–363, https://doi.org/10.1016/S0167-2991(04)80823-1.

[28] W. Fan, M. O'Brien, M. Ogura, M. Sanchez-Sanchez, C. Martin, F. Meneau, K. Kurumada, G. Sankar, T. Okubo, In situ observation of homogeneous nucleation of nanosized zeolite A, Phys. Chem. Chem. Phys. 8 (2006) 1335–1339, https://doi.org/10.1039/B510963A.

[29] G. Sankar, W. Bras, Insights into the formation of microporous materials by in situ X-ray scattering techniques, Catal. Today 145 (2009) 195–203, https://doi.org/10.1016/j.cattod.2009.05.010.

[30] J.C. Groen, G.M. Hamminga, J.A. Moulijn, J. Pérez-Ramírez, In situ monitoring of desilication of MFI-type zeolites in alkaline medium, Phys. Chem. Chem. Phys. 9 (2007) 4822–4830, https://doi.org/10.1039/b705418a.

[31] I. Halasz, M. Agarwal, R. Li, N. Miller, Monitoring the structure of water soluble silicates, Catal. Today 126 (2007) 196–202, https://doi.org/10.1016/j.cattod.2006.09.032.

[32] L. Bressel, R. Hass, O. Reich, Particle sizing in highly turbid dispersions by Photon Density Wave spectroscopy, J. Quant. Spectrosc. Radiat. Transfer 126 (2013) 122–129, https://doi.org/10.1016/j.jqsrt.2012.11.031.

[33] R. Hass, M. Münzberg, L. Bressel, O. Reich, Industrial applications of Photon Density Wave spectroscopy for in-line particle sizing, Appl. Opt. 52 (2013) 1423–1431, https://doi.org/10.1364/AO.52.001423.

[34] J.B. Fishkin, S. Fantini, M.J. vandeVen, E. Gratton, Gigahertz photon density waves in a turbid medium: Theory and experiments, Phys. Rev. E. 53 (1996) 2307–2319, https://doi.org/10.1103/PhysRevE.53.2307.

[35] S.M. Richter, R.R. Shinde, G.V. Balgi, E.M. Sevick-Muraca, Particle sizing using frequency domain photon migration, Part. Part. Syst. Char. 15 (1998) 9–15, https://doi.org/10.1002/(SICI)1521-4117(199802)15:1<9::AID-PPSC9>3.0.CO;2-X.

[36] A. Hartwig, R. Hass, Monitoring lactose crystallization at industrially relevant concentrations by Photon Density Wave spectroscopy, Chem. Eng. Technol. 41 (2018) 1139–1146, https://doi.org/10.1002/ceat.201700685.

[37] G. Mie, Beiträge zur Optik trüber Medien, speziell kolloidaler Metallösungen, Ann. Phys. 330 (1908) 377–445, https://doi.org/10.1002/andp.19083300302.

[38] S. Mintova (Ed.), Verifed Syntheses of Zeolitic Materials, Third Revised Edition, International Zeolite Association, 2016, http://www.iza-online.org/synthesis/VS_3rdEd.pdf , Accessed date: 2 July 2019.

[39] S. Vargas Ruiz, R. Hass, O. Reich, Optical monitoring of milk fat phase transition within homogenized fresh milk by Photon Density Wave spectroscopy, Int. Dairy J. 26 (2012) 120–126, https://doi.org/10.1016/j.idairyj.2012.03.012.

[40] T.B. Reed, D.W. Breck, Crystalline zeolites. II. Crystal structure of synthetic zeolite, type A, J. Am. Chem. Soc. 78 (1956) 5972–5977, https://doi.org/10.1021/ja01604a002.

[41] C. Baerlocher, L.B. McCusker, Database of Zeolite Structures, http://www.iza-structure.org/databases/ , Accessed date: 23 January 2019.

[42] S. Mintova, N.H. Olson, V. Valtchev, T. Bein, Mechanism of zeolite a nanocrystal growth from colloids at room temperature, Science 283 (1999) 958–960, https://doi.org/10.1126/science.283.5404.958.

[43] L. Gora, K. Streletzky, R.W. Thompson, G.D.J. Phillies, Study of the crystallization of zeolite NaA by quasi-elastic light-scattering spectroscopy and electron microscopy, Zeolites 18 (1997) 119–131, https://doi.org/10.1016/S0144-2449(96)00144-3.

[44] J.A. Kostinko, Factors influencing the synthesis of zeolites A, X, and Y, in: G.D. Stucky, F.G. Dwyer (Eds.), Intrazeolite Chemistry, American Chemical Society, Washington, D.C., 1983, pp. 3–19, , https://doi.org/10.1021/bk-1983-0218.ch001.

[45] S. Shirazian, S.G. Parto, S.N. Ashrafizadeh, Effect of water content of synthetic hydrogel on dehydration performance of nanoporous LTA zeolite membranes, Int. J. Appl. Ceram. Technol. 11 (2014) 793–803, https://doi.org/10.1111/ijac.12088.

[46] X. Zhang, D. Tong, W. Jia, D. Tang, X. Li, R. Yang, Studies on room-temperature synthesis of zeolite NaA, Mater. Res. Bull. 52 (2014) 96–102, https://doi.org/10.1016/j.materresbull.2014.01.008.

[47] A. Zabala Ruiz, D. Brühwiler, T. Ban, G. Calzaferri, Synthesis of zeolite L. Tuning size and morphology, Monatshefte Chem. 136 (2005) 77–89, https://doi.org/10.1007/s00706-004-0253-z.

[48] V. Gramlich, W.M. Meier, The crystal structure of hydrated NaA : a detailed refinement of a pseudosymmetric zeolite structure, Z. Kristallogr. 133 (2015) 134–149, https://doi.org/10.1524/zkri.1971.133.16.134.